

Suppression of moisture-induced embrittlement of Ni₃(Si, Ti) alloys by a surface nickel alloying layer

C. L. MA, T. TAKASUGI, S. HANADA

Institute for Materials Research, Tohoku University, Katahira 2-1-1, Aoba-ku, Sendai, 980-77, Japan

The effect of a surface nickel alloying layer on moisture-induced embrittlement of Ni₃(Si, Ti) alloys has been investigated by tensile tests at room temperature, using nickel-deposited materials. Undeposited Ni₃(Si, Ti) alloy became remarkably embrittled in air. However, nickel-deposited Ni₃(Si, Ti) alloy showed a high elongation value, indicating the suppression of embrittlement caused by hydrogen decomposed from moisture in the air. When the surface nickel alloying layer consists of fcc(γ) solid solution with a high nickel concentration and good adhesion to the substrate, improvement of tensile elongation is the greatest. The results have been discussed from the chemical and structural viewpoints of the surface nickel alloying layer.

1. Introduction

A number of ordered intermetallics have been shown to be susceptible to embrittlement due to hydrogen released from water vapour in air, as well as residual hydrogen contained in materials (see review articles [1–6]). Therefore, suppression of environmental embrittlement is an important subject in developing ordered intermetallics as engineering structural materials. Besides control or selection of “environmental” parameters (such as temperature, deformation rate or atmosphere), three kinds of techniques as “materials” parameters may be considered to alleviate this kind of embrittlement. The first technique is an alloying method and the second technique is microstructural modification, both of which can reduce embrittlement of ordered intermetallics not only during their fabrication process but also during their service lives. It has actually been shown that the alloying technique was successful in reducing the environmental embrittlement particularly in L1₂ alloys [7–13]. For example, the environmental embrittlement of Co₃Ti alloys was suppressed by the addition of a few atomic per cent of iron and aluminium elements [7, 8]. Also, the environmental embrittlement of Ni₃(Si, Ti) alloys was suppressed by a macro-alloying of chromium, manganese and iron [9, 10], and also by a micro-alloying of boron (and carbon) [11–13]. A third technique is surface modification, by which embrittlement of ordered intermetallics can be effectively alleviated during their service lives. Recently, it was shown that pre-deformed [14, 15] or shot-peened [16] Ni₃(Si, Ti) alloys have the effect of suppressing embrittlement due to hydrogen decomposed from moisture in the air [15, 16] as well as hydrogen contained as a residue

[14]. In those studies, it was suggested that hydrogen atoms can be trapped by introduced dislocations (or vacancies) and are thereby blocked to enrich to grain boundaries which are the weakest links in the L1₂ structure. Thus, the deformed microstructure was shown to result in a beneficial effect of reducing the environmental embrittlement of Ni₃(Si, Ti) alloy.

The moisture-induced embrittlement in ordered intermetallics is primarily attributed to an intensive reaction of moisture in air with a reactive element composed of alloys [17] (e.g. silicon or titanium in this Ni₃(Si, Ti) alloy) on the material surface. This reaction generates atomic hydrogen, followed by some subsequent processes (such as permeation, diffusion and condensation). This feature implies that surface chemistry is an important parameter affecting the moisture-induced embrittlement of ordered intermetallics. It is anticipated that the moisture-induced embrittlement of ordered intermetallics may be reduced if materials are coated by a surface film, the composition of which contains no reactive elements such as aluminium, silicon or titanium. Also, if the crystal structure of the surface layer is different from that of the substrate (e.g. disordered structure or pure metal) and less susceptible to hydrogen-induced embrittlement, this embrittlement may be reduced. In this work, a nickel film was electrolytically deposited on to Ni₃(Si, Ti) alloys, and annealed in a few conditions to produce different microstructures in the surface alloying layer. Ductility was evaluated by tensile tests in air at room temperature. The observed mechanical behaviour and fractography have been discussed in association with the resultant surface nickel alloying layer.

2. Experimental procedure

$\text{Ni}_3(\text{Si}, \text{Ti})$ alloys with a nominal composition of $\text{Ni}_{79.5}\text{Si}_{11}\text{Ti}_{9.5}$ (atomic per cent) were prepared by a non-consumable arc melting technique in argon gas on a copper hearth. The purity of the raw materials was 99.9 wt% Ni, 99.999 wt% Si and 99.9 wt% Ti. Alloy ingot buttons with dimensions 50 mm \times 30 mm \times 15 mm were homogenized at 1323 K for 1 d in a vacuum, and then cut into several pieces parallel to the solidification direction of the button ingot. These pieces were then repeatedly rolled at room temperature and annealed in a vacuum at 1273 K for 5 h. Tensile specimens with a gauge dimension of 14 mm \times 2 mm \times 1 mm were prepared by an electro-discharge machine (EDM) from rolled plates, and then annealed at 1273 K for 5 h in a vacuum to obtain a recrystallized microstructure with fully ordered structure. The surfaces of the tensile specimens were then abraded on SiC paper. The average grain diameter, measured by the linear intercept method, was about 40 μm .

The tensile specimens were electro-polished in a solution of 15 vol% H_2SO_4 and 85 vol% CH_3OH at 280 K. The electro-deposition of the nickel film was then carried out at 285 K in a Watt bath (nickel sulfate, 300 g l^{-1} ; nickel chloride, 45 g l^{-1} ; and boric acid, 35 g l^{-1}). The desired thickness of the nickel film was obtained from predetermined deposition time versus thickness relations where the film thickness was determined by a weighing method. Some of the nickel-deposited specimens were annealed in a vacuum at 673 K for 5 h and 1273 K for 5 h. The surface nickel alloying layer was characterized using optical microscopy (OM), X-ray diffraction (XRD) and electron probe microscopic analysis (EPMA). Compositional variation for each constituent element, nickel, silicon and titanium, with depth from the specimen surface was determined using their K_α radiation.

Tensile tests were conducted at room temperature at an initial strain rate of $5.9 \times 10^{-5} \text{ s}^{-1}$ in laboratory air (with a relative humidity of about 60%–80%), using an Instron-type machine. Most specimens were deformed up to fracture. Fracture surfaces and side surfaces of the tested specimens were examined by scanning electron microscopy (SEM) and OM.

3. Results

3.1. Characterization of the surface nickel alloying layer

Figs 1 and 2 show SEM images and concentration variations of the constituent elements with the depth from the surface in $\text{Ni}_3(\text{Si}, \text{Ti})$ alloys which have different microstructures in the surface nickel alloying layer. For an $\text{Ni}_3(\text{Si}, \text{Ti})$ alloy which has a 15 μm initial thickness of nickel film and was annealed at 673 K for 5 h (Fig. 2a), the nickel concentration at the specimen surface was 100% Ni and almost constant up to the immediate vicinity of the substrate, while the nickel concentration in the substrate adjoining the nickel film (i.e. γ phase) slightly increased to 81% Ni. For an $\text{Ni}_3(\text{Si}, \text{Ti})$ alloy which has an initial nickel film thick-

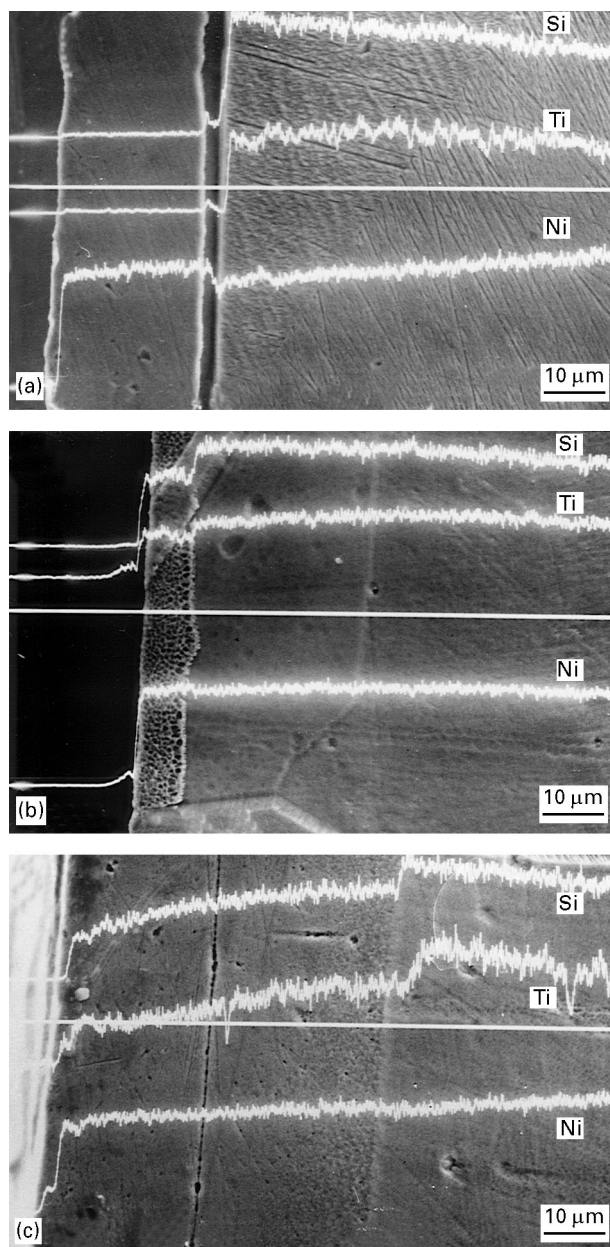


Figure 1 SEM images and line profiles of constituent elements, nickel, silicon and titanium in $\text{Ni}_3(\text{Si}, \text{Ti})$ alloys, with (a) an initial thickness of 15 μm nickel film and annealed at 673 K for 5 h, (b) an initial thickness of 6 μm nickel film and annealed at 1273 K for 5 h, and (c) an initial thickness of 15 μm nickel film and annealed at 1273 K for 5 h, respectively.

ness of 6 μm and was annealed at 1273 K for 5 h (Fig. 2b), interdiffusion was apparent; the nickel concentration in the surface alloying layer decreased and was constant (i.e. 81.5% Ni). Its concentration value was equilibrated to 79.5% Ni in the substrate adjoining the nickel film (i.e. γ phase). For an $\text{Ni}_3(\text{Si}, \text{Ti})$ alloy which has an initial nickel film thickness of 15 μm and was annealed at 1273 K for 5 h (Fig. 2c), the nickel concentration at the specimen surface was 85% Ni and gradually decreased on approaching an interface (γ/γ'). At an interface, 81.5% Ni in the γ phase was equilibrated to 79.5% Ni in the γ' phase. Thus, the observed phase and concentration relations seem to be consistent with metallographic observations previously reported in the Ni–Si–Ti alloy system [18, 19].

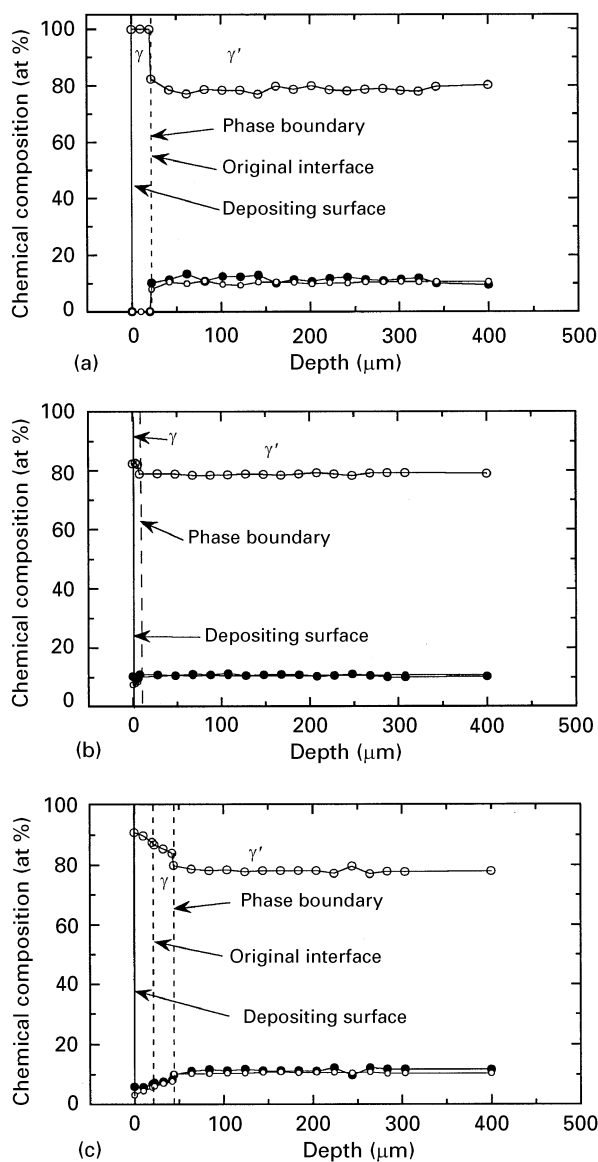


Figure 2 Concentration variations of constituent elements, (○) nickel, (●) silicon and (●) titanium with depth from surface of $\text{Ni}_3(\text{Si}, \text{Ti})$ alloys, with (a) an initial thickness of 15 μm nickel film and annealed at 673 K for 5 h, (b) an initial thickness of 6 μm nickel film and annealed at 1273 K for 5 h, and (c) an initial thickness of 15 μm nickel film and annealed at 1273 K for 5 h, respectively.

Here, it should be noted that the surface nickel alloying layer did not consist of γ' phase (i.e. L1_2 ordered structure) but of nickel solid solution (i.e. γ phase: fcc disordered structure) even though the annealing was carried out under conditions of high temperature, longer time and thin film. This is because the alloy composition of $\text{Ni}_3(\text{Si}, \text{Ti})$ substrate used in this study was very close to the solubility limit of γ phase in γ' phase [18, 19], and consequently enrichment of the nickel concentration in the γ' phase (i.e. $\text{Ni}_3(\text{Si}, \text{Ti})$ substrate) was not so much required in interdiffusion.

3.2. Mechanical behaviour and fractography

Fig. 3 shows nominal stress–nominal strain curves of $\text{Ni}_3(\text{Si}, \text{Ti})$ alloys which were electro-deposited and

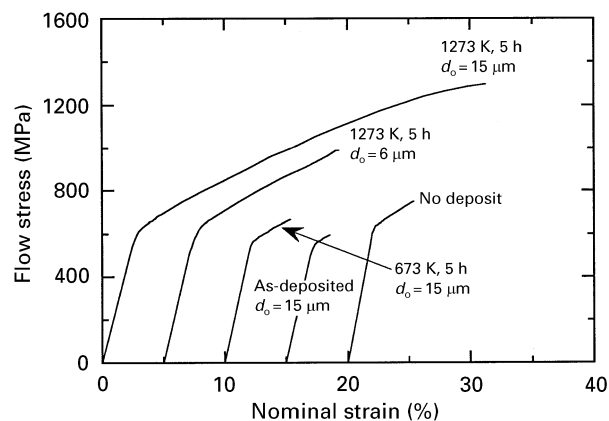


Figure 3 Nominal stress–nominal strain curves of $\text{Ni}_3(\text{Si}, \text{Ti})$ alloys which were electro-deposited and annealed under various conditions. Results of an undeposited $\text{Ni}_3(\text{Si}, \text{Ti})$ alloy are also included for comparison.

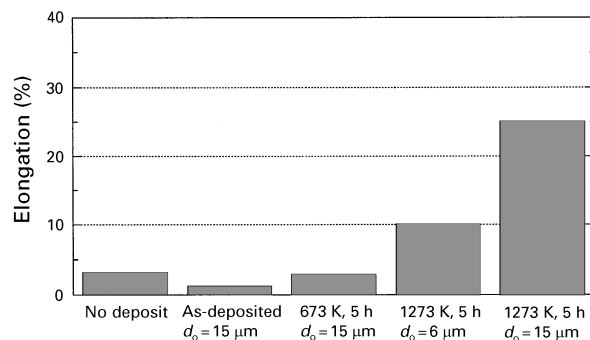


Figure 4 Comparison of tensile elongation measured in $\text{Ni}_3(\text{Si}, \text{Ti})$ alloys which were electro-deposited and annealed under various conditions. Results of an undeposited $\text{Ni}_3(\text{Si}, \text{Ti})$ alloy are also included for comparison.

annealed under various conditions, together with the result of undeposited $\text{Ni}_3(\text{Si}, \text{Ti})$ alloy. An undeposited $\text{Ni}_3(\text{Si}, \text{Ti})$ alloy showed a low tensile elongation of about 3%. An as-deposited $\text{Ni}_3(\text{Si}, \text{Ti})$ alloy with 15 μm nickel film showed slightly lower tensile elongation (i.e. about 2%) than the undeposited $\text{Ni}_3(\text{Si}, \text{Ti})$ alloy. On the other hand, an $\text{Ni}_3(\text{Si}, \text{Ti})$ alloy (with an initial nickel film thickness of 15 μm) annealed at 673 K for 5 h, showed a tensile elongation of about 3%, being primarily identical to that of the undeposited $\text{Ni}_3(\text{Si}, \text{Ti})$ alloy. However, $\text{Ni}_3(\text{Si}, \text{Ti})$ alloys (with initial nickel film thicknesses of 6 and 15 μm) annealed at 1273 K for 5 h showed high elongation values, i.e. 10% and 25%, respectively. The observed tensile elongation of 25% is close to the tensile elongation ($\sim 30\%$) in the $\text{Ni}_3(\text{Si}, \text{Ti})$ alloy deformed in a vacuum at room temperature [9, 13–16]. Fig. 4 summarizes the observed tensile elongation of the $\text{Ni}_3(\text{Si}, \text{Ti})$ alloys with different microstructure in the surface nickel alloying layer. It is thus evident that the surface alloying layer consisting of nickel solid solution (γ phase) has the effect of suppressing the embrittlement caused by hydrogen released from moisture in the air.

Fig. 5 shows SEM fractography of the undeposited $\text{Ni}_3(\text{Si}, \text{Ti})$ alloy. It is obvious that the fracture surface

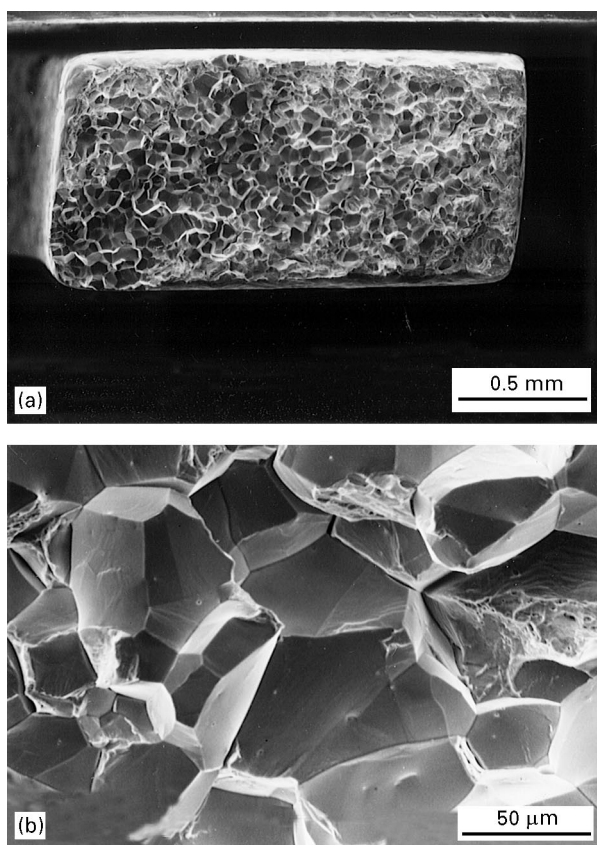


Figure 5 (a, b) SEM fractography of an undeposited $\text{Ni}_3(\text{Si, Ti})$ alloy.

consisted of intergranular fracture and is therefore consistent with the mechanical behaviour result shown in Figs 3 and 4; low tensile elongation is due to the intergranular fracture. Fig. 6 shows SEM fractography of $\text{Ni}_3(\text{Si, Ti})$ alloys which have different initial nickel film thicknesses and were annealed under different conditions. For the $\text{Ni}_3(\text{Si, Ti})$ alloy, which has an initial thickness of 15 μm nickel film and was annealed at 673 K for 5 h (Fig. 6a, b), the SEM fractograph showed intergranular fracture, being therefore similar to that observed in the undeposited $\text{Ni}_3(\text{Si, Ti})$ alloy. For the $\text{Ni}_3(\text{Si, Ti})$ alloy which had an initial nickel film thickness of 6 μm and was annealed at 1273 K for 5 h (Fig. 6c, d), the SEM fractograph showed intergranular fracture with a minority area fraction of transgranular fracture. For the $\text{Ni}_3(\text{Si, Ti})$ alloy which has an initial thickness of 15 μm nickel film and was annealed at 1273 K for 5 h (Fig. 6e, f), almost equal area fractions of intergranular fracture and transgranular fracture were seen in the SEM fractograph. In the latter two $\text{Ni}_3(\text{Si, Ti})$ alloys, the transgranular fracture pattern appears to be more prevalent in the outer region of the specimen, indicating that the surface nickel alloying layer is effective in suppressing intergranular fracture. Thus, the observed SEM fractography was consistent with the tensile elongation behaviour shown in Figs 3 and 4; ductile transgranular fracture mode results in a high elongation value.

4. Discussion

As mentioned in Section 1, the beneficial effect of a surface nickel alloying layer on the moisture-induced embrittlement of $\text{Ni}_3(\text{Si, Ti})$ alloys can firstly be attributed to its chemical nature. In the surface nickel alloying layer, the concentration of active elements such as silicon and titanium is lower than that in the substrate. This feature implies that a decomposition process based on a reaction $\text{Ni}_3(\text{Si, Ti}) + \text{H}_2\text{O} \rightarrow 3\text{Ni} + \text{Si (or Ti) O} + 2\text{H}$ [17] is reduced, and thereby subsequent hydrogen kinetics (e.g. absorption, diffusion and condensation) can be suppressed. As a result, electro-deposited $\text{Ni}_3(\text{Si, Ti})$ alloys become resistive to the moisture-induced embrittlement. Secondly, the beneficial effect of the surface nickel alloying layer may be attributed to its structural feature. All of the surface nickel alloying layer prepared in this study consisted of disordered fcc structure (i.e. γ phase). It has widely been observed that ordered alloy (structure) is more susceptible to the hydrogen-induced embrittlement than the corresponding disordered alloy (structure). For example, ordered Ni_3Fe alloy has been shown to be very susceptible to embrittlement due to hydrogen-gas exposure at room temperature, while disordered Ni_3Fe alloy showed little susceptibility to this kind of embrittlement [20, 21]. As a possible explanation for this difference in the hydrogen-induced embrittlement between ordered and disordered fcc structures, it has been suggested that grain boundaries in the ordered structure are less accommodated and therefore have large free volumes [22]. Consequently, atomic hydrogen can largely occupy their sites on grain boundaries, and this results in easier intergranular fracture. Also, dislocations and point defects (such as vacancies) introduced into the surface nickel alloying layer (due to residual stress or inter diffusion) may affect hydrogen kinetics and modify the mechanical property of the substrate as well as the surface nickel alloying layer [14–16], thereby reducing the hydrogen embrittlement susceptibility.

However, the tensile ductility of electro-deposited $\text{Ni}_3(\text{Si, Ti})$ alloys was very dependent on the micro-structure formed in the surface nickel alloying layer. The tensile elongation of the as-deposited $\text{Ni}_3(\text{Si, Ti})$ alloy was rather slightly lower than the undeposited $\text{Ni}_3(\text{Si, Ti})$ alloy. This may be due to the hydrogen involved from a Watt solution during electro-deposition. It appears that the high concentration of hydrogen contained in the electro-deposited nickel film was harmful and reduced tensile ductility. Also, when interdiffusion (i.e. alloying) in the surface nickel film layer was not so intensive (e.g. in the $\text{Ni}_3(\text{Si, Ti})$ alloy annealed at 473 K for 5 h), the improvement in the tensile elongation was not significant. OM observation on the side surface of the fractured specimen showed that a number of cracks occurred in the nickel film and also peeling between the nickel film and the substrate took place. This degradation of the nickel film by deformation was also observed in the case of the as-deposited $\text{Ni}_3(\text{Si, Ti})$ alloy. In such a situation, hydrogen can be easily absorbed through cracked paths and also peeled voids, and the surface nickel alloying layer becomes less protective from the

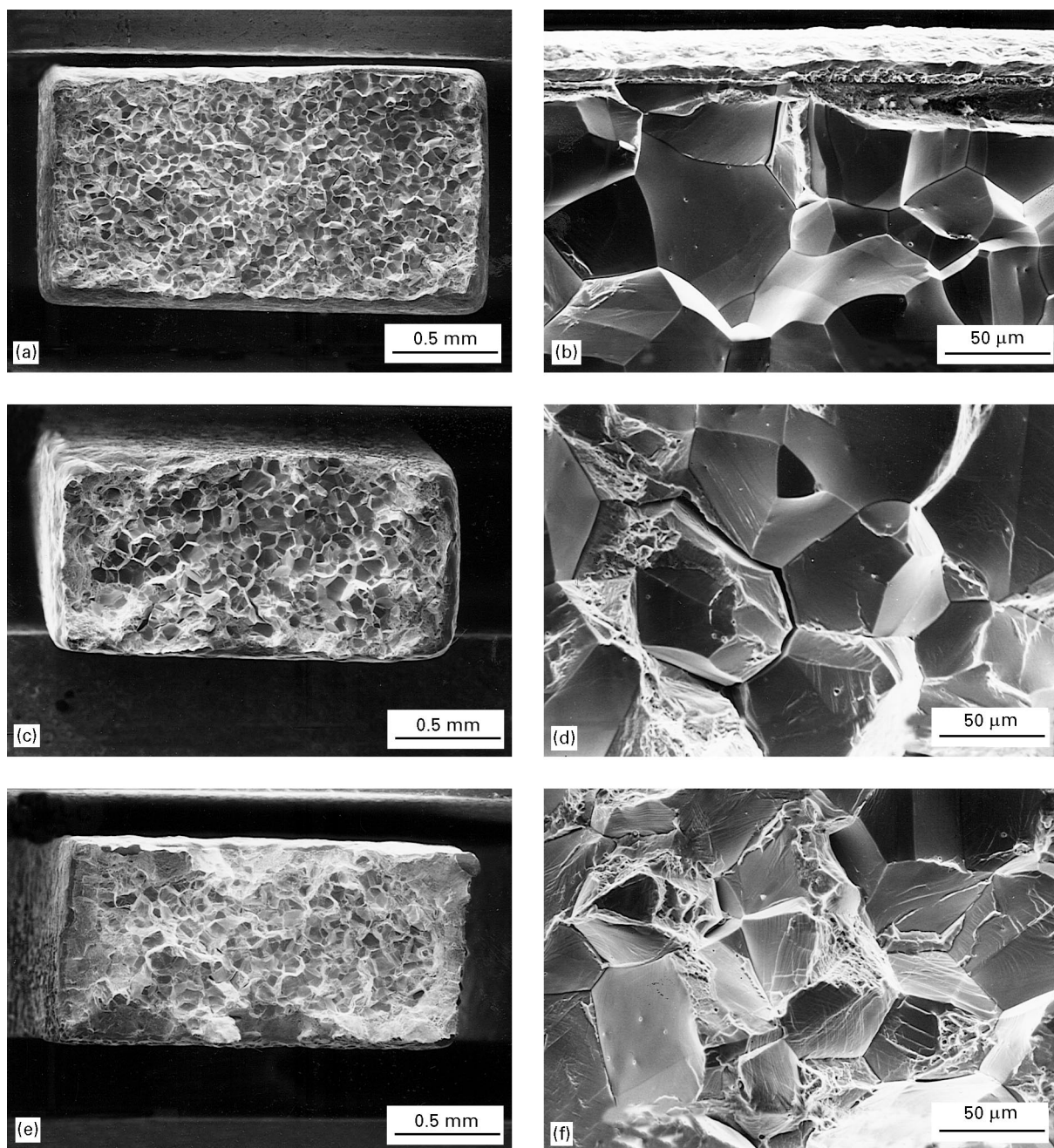


Figure 6 SEM fractographic comparison of $\text{Ni}_3(\text{Si}, \text{Ti})$ alloys with (a, b) an initial thickness of $15 \mu\text{m}$ nickel film and annealed at 673 K for 5 h , (c, d) an initial thickness of $6 \mu\text{m}$ nickel film and annealed at 1273 K for 5 h , and (e, f) an initial thickness of $15 \mu\text{m}$ nickel film and annealed at 1273 K for 5 h , respectively.

moisture-induced embrittlement. When the surface nickel alloying layer consisted of a high nickel concentration at its surface and relatively large thickness (i.e. in the $\text{Ni}_3(\text{Si}, \text{Ti})$ alloy annealed at 1273 K for 5 h and with an initial thickness of $15 \mu\text{m}$), the improvement in the tensile ductility was the greatest. OM and SEM observations on the fractured specimen indicated little cracking in the surface nickel alloying layer and no peeling between substrate and film. In this case, it appears that the surface nickel alloying layer protected against decomposition and subsequent absorption process of hydrogen.

Finally, from the point of view of application, the nickel deposition layer may be inappropriate to protect ordered intermetallics from the moisture-induced embrittlement. A number of ordered intermetallics are expected to be utilized in corrosive environments and

at high temperatures. The surface nickel alloying layer prepared in this study seems to be less protective to corrosion at low temperature and to oxidation at high temperature. Also, nickel can quickly diffuse into the substrate in a brief time and therefore the stability of the nickel film is not so good. Accordingly, coating materials and techniques by which ordered intermetallics can achieve high resistance to environmental embrittlement, should be studied and developed.

5. Conclusion

The effect of a surface nickel alloying layer on moisture-induced embrittlement of $\text{Ni}_3(\text{Si}, \text{Ti})$ alloys was investigated by tensile tests at room temperature. Undeposited $\text{Ni}_3(\text{Si}, \text{Ti})$ alloy was remarkably embrittled in air while the $\text{Ni}_3(\text{Si}, \text{Ti})$ alloy with a surface

nickel alloying layer showed high tensile elongation in air. When the surface nickel alloying layer consisted of fcc(γ) solid solution with a high nickel concentration and good adhesion to the substrate, improvement of tensile elongation was the greatest. Results have been discussed from the chemical and structural viewpoints of the surface nickel alloying layer.

Acknowledgements

This work was supported in part by the Grant-in-aid for Scientific Research from the Ministry of Education, Science and Culture. The authors thank Mr. H. Suenaga for tensile testing.

References

1. T. TAKASUGI and O. IZUMI, *Mater. Forum* **12** (1988) 8.
2. *Idem*, "High-Temperature Ordered Intermetallic Alloys IV", MRS Symposium Proceedings Publication, Vol. 213 edited by L. Johnson, D. P. Pope and J. O. Stiegler, (MRC, Pittsburgh PA, 1991) p. 403.
3. *Idem*, in "Critical Issues in the Development of High Temperature Structural Materials", edited by N. Stoloff, D. J. Duquette and A. F. Giamei (Minerals, Metals and Materials Society, Warrendale, PA, 1993) p. 399.
4. C. T. LIU, in "6th International Symposium on Intermetallic Compounds – Structure and Mechanical Properties", edited by O. Izumi (JIM, Sendai, Japan, 1991) p. 703.
5. *Idem*, in "Ordered Intermetallics – Physical Metallurgy and Mechanical Behavior", edited by C. T. Liu, R. W. Cahn and G. Sauthoff (Kluwer Academic, 1992) p. 321.
6. E. P. GEORGE and C. T. LIU, in "High-Temperature Ordered Intermetallic Alloys VI", MRS Symposium Proceedings Publication, Vol. 364 (1995) p. 1131.
7. Y. LIU, T. TAKASUGI and O. IZUMI, *J. Mater. Sci.* **24** (1989) 4458.
8. A. KIMURA, H. IZUMI, T. MISAWA and H. SAITOH, *Mater. Trans. JIM* **35** (1994) 879.
9. C. L. MA, T. TAKASUGI and S. HANADA, *Scripta Metall. Mater.* **32** (1995) 1025.
10. *Idem*, in "High-Temperature Ordered Intermetallic Alloys VI", MRS Symposium Proceedings Publication, edited by J. Horton, I. Baker, S. Hanada, R. D. Noebe and D. Schwarz, Vol. **364** (MRC, Pittsburgh PA, 1995) p. 1159.
11. T. TAKASUGI, H. SUENAGA and O. IZUMI, *J. Mater. Sci.* **26** (1991) 1179.
12. T. TAKASUGI and M. YOSHIDA, *ibid.* **26** (1991) 3032.
13. C. L. MA, T. TAKASUGI and S. HANADA, *Mater. Trans. JIM* **36** (1995) 30.
14. *Idem*, *Acta Metall. Mater.*, **44** (1996) 1349.
15. *Idem*, *Scripta Metall. Mater.*, **34** (1996) 1633.
16. *Idem*, *ibid.*, **34** (1996) 1131.
17. C. T. LIU, E. H. LEE and C. G. McKAMEY, *Scripta Metall.* **23** (1989) 875.
18. K. J. WILLIAMS, *J. Inst. Metals* **99** (1971) 310.
19. T. TAKASUGI, D. SHINDO, O. IZUMI and M. HIRABAYASHI, *Acta Metall. Mater.* **38** (1990) 739.
20. T. TAKASUGI, T. EGUCHI, M. YOSHIDA and O. IZUMI, *J. Jpn Inst. Metals* **53** (1989) 34.
21. *Idem*, *ibid.* **53** (1989) 42.
22. J. J. KRUISMAN, V. VITEK and J. Th. DeHOSSON, *Acta Metall.* **36** (1988) 2729.

*Received 8 December 1995
and accepted 10 March 1997*